# PREPARATION AND CHARACTERIZATION OF $Al_2O_3/SiO_2/Si$ TUNNEL DIODE

Zaw Win[1]

## Abstract

Aluminum oxide ($Al_2O_3$) moisture less powder was formed by mixing aluminum nitrate nonahydrate (Al $(NO_3)_3.9H_2O$) and glycine ($C_2H_5NO_2$) via auto combustion method. X-ray diffraction (XRD) and Scanning Electron Microscope (SEM) techniques were used to examine the structure and microstructural properties of $Al_2O_3$ powder. The structure of $Al_2O_3/SiO_2/Si$ cell exhibited the schottky barrier height and could not indicate the tunnel diode nature. Thus, the $P_2O_5$ insertion layer was added onto the $SiO_2$ layer. Phosphorus ($P_2O_5$) diffusion was made on the $SiO_2$/p-Si (100) substrate and annealed at 550 $^{o}$C for 1 h to form $p^+$ p design. The SEM was employed to observe the surface morphology and thickness of $P_2O_5$ layer. The $Al_2O_3$ sol-solution was deposited onto $P_2O_5/SiO_2/Si$ substrate by spin coating technique. The microstructure and film thickness of $Al_2O_3$ layer were also examined by SEM. The charge conduction mechanism of $Al_2O_3$ film was identified by $C^{-2}$-V characteristics. The change in peak current and the valley current with respect to annealing temperatures were studied.

**Keywords:** XRD Analysis of $Al_2O_3$ Powder and SEM Analysis of $P_2O_5$/Si Layer

## Introduction

A tunnel diode is a type of semiconductor diode that is capable of very fast operation, well into the microwave frequency region, by using the quantum mechanical effect called tunneling. Tunnel diode is p-n junction device that exhibits negative resistance. That means when the voltage is increased the current through it decreases. They are used in frequency converters and detectors. They have negative differential resistance in part of their operating range, and therefore are also used as oscillators, amplifiers and in switching circuits using hysteresis. Aluminum is one of the most important materials because of its high strength and modulus, resistance to attacks from molten metals and non-oxide materials, chemical inertness in both oxidizing and reducing atmospheres up to 1000°C, and good electrical insulation. Aluminum also has high melting point ($t_m$> 2040°C) and low thermal conductivity (10-18 W/ (mK)). An important potential application of alumina is as fiber reinforcement of metals, ceramics and resins.

## Experimental Procedure

### Samples Preparation

P-type silicon with (100) orientation was cleaned by standard silicon cleaning process. First of all, Phosphorus (P2O5) was dissolved in methoxythanol (2-CH3OCH2CH2OH) and deposited onto p-Si (100) substrates by spin coating technique. It was annealed at 550 oC for 1h to form p+ p design. Aluminum nitrate [Al (NO3)3.9H2O] and glycine (C2H5NO2) were used as starting chemicals with analytical grade. Aluminum nitrate nonahydrate and glycine (1:3) were mixed and a small amount of ammonium hydroxide (NH4OH) was added to the solution to change the neutral solution. During the process, the solution was stirred and heated at 60 oC for 8 h. Next, it was aged in air atmosphere for 12 h and jelly-like solution was formed. To get the dried gel, the jelly-like solution was dried at 90 oC for 1h and dried gel was formed. It was poured into crucible and heated at 400 oC for 30 min. Thus, Al2O3 powder was obtained and it was annealed at 1100 oC for 3 h for move crystalline fine and moisture-less. The Al2O3 powder and 2-CH3OCH2CH2OH solvent were mixed and refluxed at 110oC for 3h. After air cooling, transparent Al2O3 sol solution was formed and ready to deposit onto p+ p substrate. It was coated onto p+ p substrate by single wafer spin

[1] Physics Department, Yadanabon University

processor. To change from coating layer into oxide film, they were annealed at 500 oC, 600 oC and 700 oC for 1 h. Figure (1) shows the flow chart of preparation for AL2O3 precursor solution

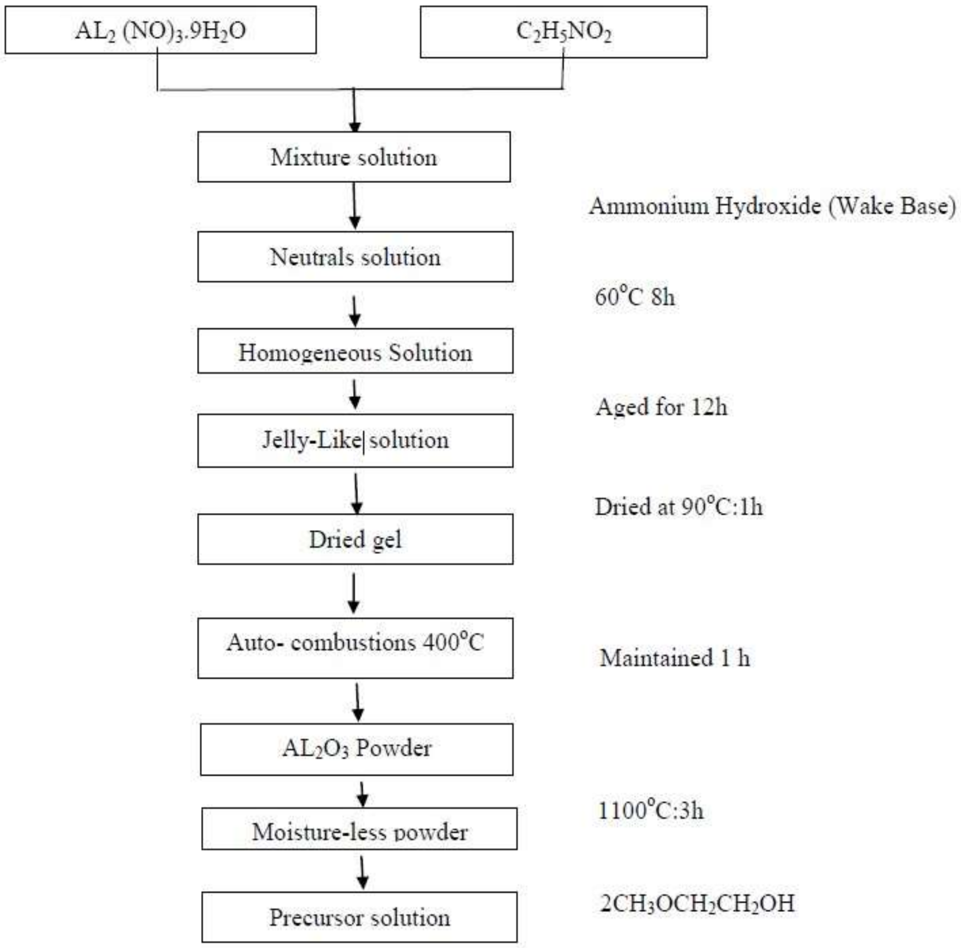


**Figure 1.** Flow chart of preparation for $AL_2O_3$ precursor solution

## Results and Discussion

### XRD Analysis of Al2O3 Powder

XRD analysis was employed to study the crystal structure and crystallographic properties of Al2O3 powder. The observed XRD profile was shown in Fig 2. The standard/reference XRD spectrum was 78-2427>Al2O3 library file (JCPDS). There was eleven peaks on observed XRD spectrum. Nine of eleven were matched well with that of standard spectrum. The crystal structure was examined to be hexagonal symmetry. The crystallite size of the (hkl) plane formed on observed XRD profile was calculated and collected in Table 1. The mean crystallite size (nanoparticle size) was found to be 70.3 nm. The lattice parameters (a-axis and c-axis) and hexagonality (lattice distortion) (lattice strain) (lattice micro strain) (c/a) were also evaluated and quoted in Table 2. The mean a-axis, c-axis and c/a were 4.7 Å, 12.99 Å and 2.73, respectively.

## Microstructural Properties of Al2O3 powder

The grain morphology at Al2O3 powder was examined by scanning electron microscopy (SEM). Fig 3 showed the SEM photograph of Al2O3 powder. From the figure, it was found that it exhibited elongated shape with average grain size estimated by well-known bar code system about 2.02 µm. It was found a porous microstructure and low dense. Oxide layer (P2O5 layer) (insulting layer) (buffer layer) was thermally formed on p-Si substrate (550 oC for 1 h). The surface morphology of P2O5 layer was shown in Fig 4 and Fig 5 indicated the cross-sectional view of P2O5layer. The layer thickness was found to be 0.70 µm.

## Microstructural Properties of Al2O3 film

Figure 6 (a-c) showed the SEM photographs of Al2O3 ultrafine powders at different annealing temperatures. As the detail analysis of SEM image, it was found that flat and non-cracked. This image consisted of circular features known as rosette structure in microstructure. The temperatures dependent of grain size for Al2O3 film were 0.6 $\mu$m, 0.5 $\mu$m, and 0.43 $\mu$m, respectively. It was found that grain sizes were more uniform at the increasing temperature 500 oC, 600 ºC and 700 ºC. Both microstructures were oriented toward right side and uniform grain distributions were clearly observed. The grain size with respect to the annealing temperature was plotted in Fig 7. The film thickness was found to be 36.9 µm, 29.9 µm and 24.0 µm for the Al2O3 / P2O5/SiO2/Si film at 500 ºC, 600 ºC and 700 ºC. The grain size with respect to the annealing temperature was plotted in Fig 8. The cross - sectional SEM image of Al2O3 / P2O5 /SiO2/Si film was given in Fig 9 (a-c).

## 1/C2-V Characteristics

To examine the film qualification of MIS tunnel diode, C-2-V characteristics were essentially observed. Fig 10 (a-c) gave C-2-V characteristics of MIS structure. This curve obeyed the Mott-Schottky relationship C-2-V characteristics were considered at negative bias condition because the built-in-voltage (the voltage across the space charge layer) must be positive. Thus, the built-in-voltage was obtained by extrapolating the C-2-V linear relationship. Table 3 showed the some important parameters of MIS tunnel diode.

## I-V characteristics of Si- based Tunnel Diode

The change in current as a function of DC applied voltage for tunnel diode was plotted as Figure 11. Three distinct regions were formed on I-V curve. The current was not allowed to flow at zero bias. There was no remarkable forward current through the junction at the low voltage region. It might be due to the potential barrier was still very high. The direct tunneling current started growing at 0.03 V because the electrons in the conduction of the n-region would tunnel to the empty state of the valence in p-region. Therefore, the direct tunnel current could flow at the junction from 0.03 V to 0.165 V ~ 0.195 V. At the second state, the tunnel current decreased with increase in DC applied voltage. Thus, the region was called NDR (negative differential resistance) region because it exhibited the negative slope and varied wit R= -1/slope. At the third state, the diffusion current could easily flow at the junction and it increased growing with increasing dc applied voltage. For I-V curve, it was observed that the tunnel current varied with DC voltage as following equation.

$$I_{tunnel} = \frac{V}{R_o} \exp\left[\left(-\frac{V}{V_o}\right)^m\right] \qquad (1)$$

Table 4 showed current and voltage characteristics of Si-based tunnel diode at different temperatures. Figure 12 (a) showed the change in peak current and valley current as a function of different annealing temperature. From the figure, it was found that the peak current and voltage gradually increased with an increase in annealing temperature in Table 5. Annealing temperature dependence of peak voltage and valley voltage of fabricated tunnel diode was described in Figure 12 (b) and collected in Table 6. The variation nature of this graph was examined to be reversed in that of peak and valley current. This fact indicated that the formation of tunnel diode.

**Table 1. Crystallite size of different peaks**

| Different peaks | G (nm) |
|---|---|
| (012) | 45.7 |
| (104) | 80.1 |
| (110) | 98.7 |
| (113) | 75.6 |
| (202) | 77.7 |
| (024) | 99.2 |
| (116) | 70.7 |
| (211) | 52.9 |
| (122) | 70.9 |
| (214) | 67.3 |
| (300) | 37.4 |
| Means crystalline size | 70.3 |

**Table 2. a-axis, c-axis and c/a of some observed peaks**

| Different peaks | a-axis (Å) | c-axis (Å) | c/a |
|---|---|---|---|
| 024 | 4.76 | 12.87 | 2.70 |
| 110 | 4.71 | 13.22 | 2.80 |
| 202 | 4.75 | 12.99 | 2.73 |
| 113 | 4.76 | 12.89 | 2.70 |
| Means values | 4.74 | 12.99 | 2.73 |

**Table 3. Some important diode parameters**

| Temp ($^{o}$C) | $N_a$ (cm$^{-3}$) | $N_d$ (cm$^{-3}$) | W (×10$^{-7}$ cm) | $V_{bi}$ (V) | φ (eV) |
|---|---|---|---|---|---|
| 500 | 1.26E+22 | 2.47E+04 | 4.80 | 0.366 | 3.08E-01 |
| 600 | 4.34E+21 | 4.31E+03 | 8.21 | 0.293 | 2.63E-01 |
| 700 | 4.02E+21 | 6.64E+02 | 8.58 | 0.402 | 2.14E-01 |

**Table 4. Current and voltage characteristics of Si-based tunnel diode at different temperatures**

| Voltage (V) | Current(μA) | Voltage(V) | Current(μA) | Voltage(V) | Current(μA) |
|---|---|---|---|---|---|
| 0 | 2.77 | 0.02 | 0.87 | 0.03 | 0.24 |
| 0.03 | 14.10 | 0.04 | 10.95 | 0.06 | 7.80 |
| 0.06 | 27.28 | 0.08 | 21.25 | 0.09 | 15.22 |
| 0.13 | 30.47 | 0.14 | 24.13 | 0.15 | 17.79 |
| 0.20 | 30.32 | 0.21 | 24.15 | 0.22 | 17.98 |
| 0.26 | 24.47 | 0.27 | 19.69 | 0.28 | 14.91 |
| 0.33 | 15.94 | 0.33 | 13.13 | 0.34 | 10.32 |
| 0.40 | 6.72 | 0.40 | 6.09 | 0.41 | 5.46 |
| 0.46 | 2.23 | 0.47 | 1.17 | 0.47 | 0.11 |
| 0.53 | 1.84 | 0.53 | 2.78 | 0.53 | 3.73 |
| 0.60 | 4.09 | 0.60 | 5.22 | 0.60 | 6.35 |

**Table 5. Peak current and valley current at different temperatures**

| Temperature °C | Peak current (μA) | Valley current (μA) |
|---|---|---|
| 700 | 30.47 | 2.23 |
| 600 | 24.15 | 1.17 |
| 500 | 17.98 | 0.11 |

**Table 6. Peak voltage and valley voltage at different temperatures**

| Temperature °C | Peak voltage (V) | Valley Voltage (V) |
|---|---|---|
| 700 | 0.16 | 0.46 |
| 600 | 0.17 | 0.47 |
| 500 | 0.19 | 0.47 |

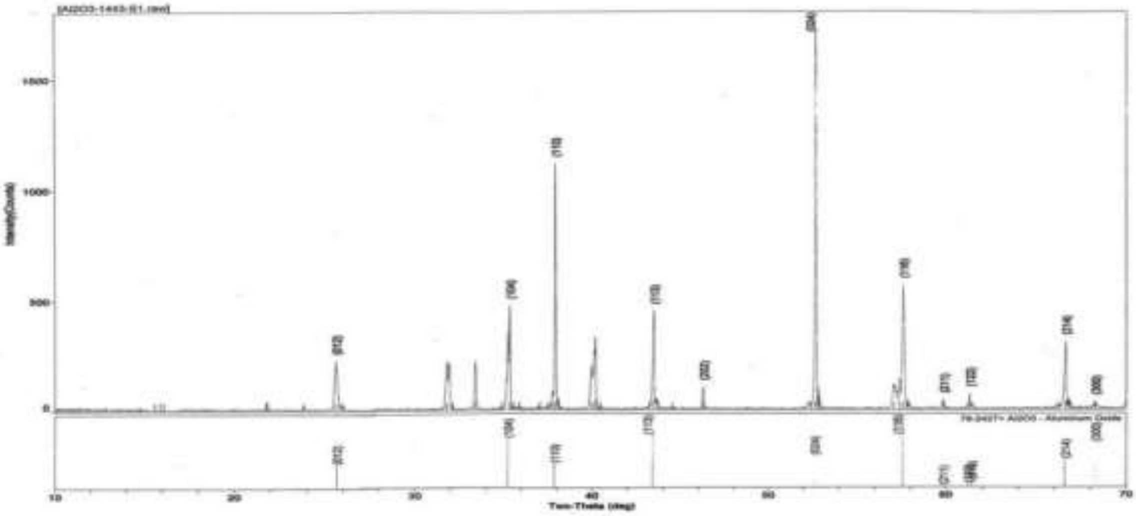

**Figure 2.** The XRD spectrum of $Al_2O_3$ ultra-fine powder

**Figure 3.** SEM photograph of $Al_2O_3$ powder

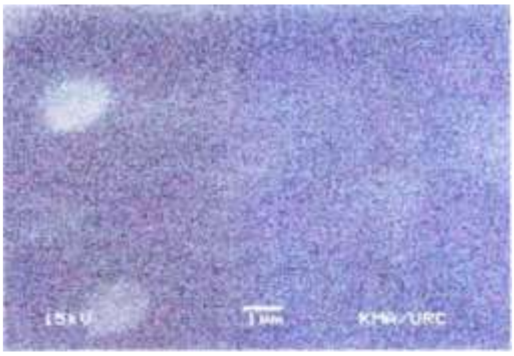

**Figure 4.** The surface morphology of $P_2O_5$ layer

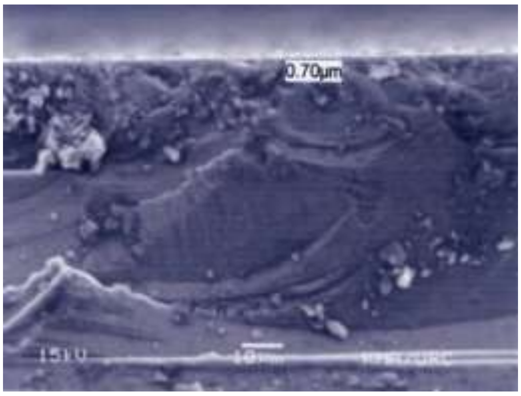


**Figure 5**. The cross-sectional view of $P_2O_5$ layer

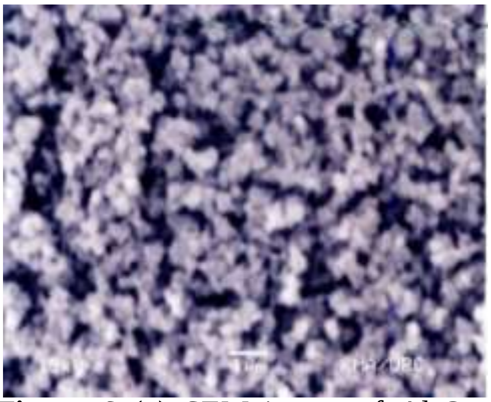

**Figure 6 (a)** SEM image of $Al_2O_3$ film at 500 ºC

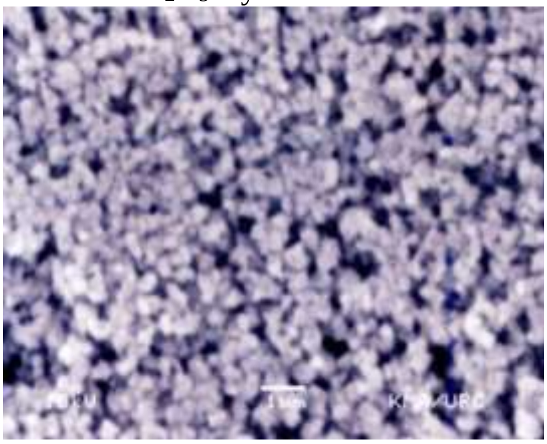

**Figure 6 (b).** SEM image of $Al_2O_3$ film at 600 ºC

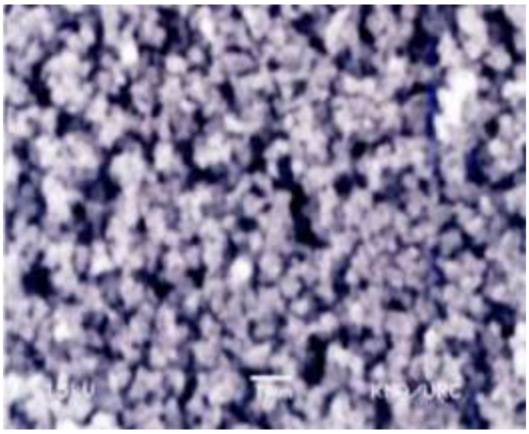

**Figure 6 (c).** SEM image of $Al_2O_3$ film at 700 ºC

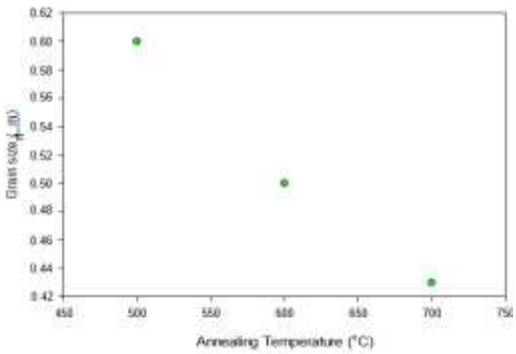


**Figure 7.** Annealing temperature dependence of grain size of $Al_2O_3$ film

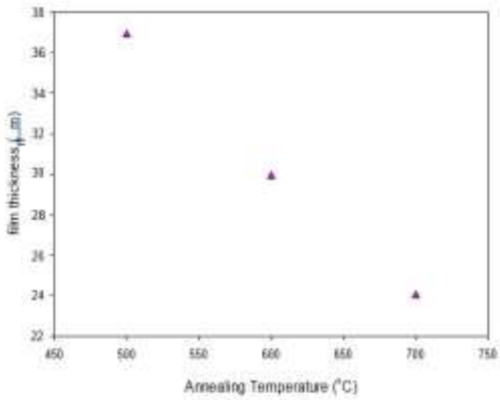


**Figure 8.** Annealing temperature dependence of grain size of $Al_2O_3$ film

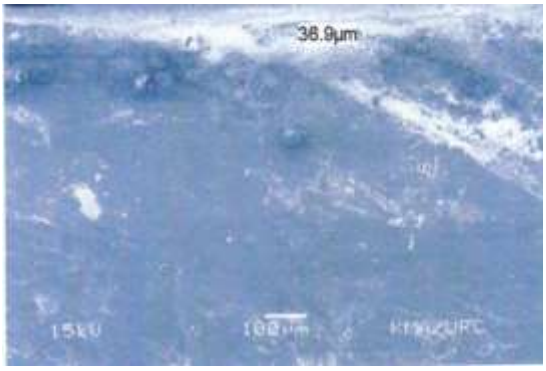


**Figure 9 (a).** The cross-sectional view of $Al_2O_3$ layer at 500 °C

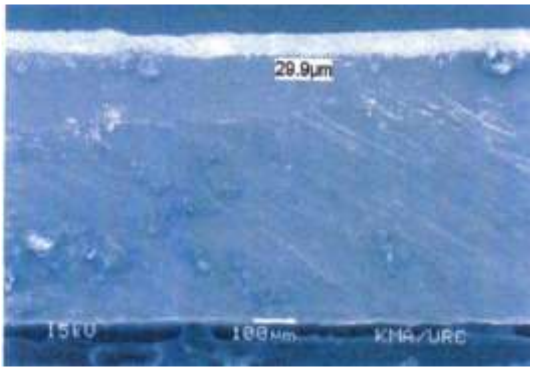


**Figure 9 (b).** The cross-sectional view of $Al_2O_3$ layer at 600 °C

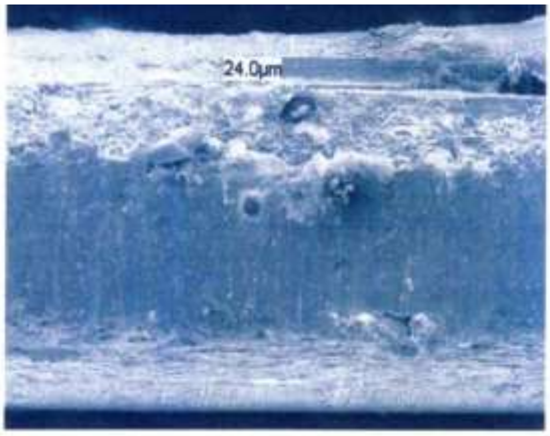


**Figure 9 (c).** The cross-sectional view of $Al_2O_3$ layer at 700 °C

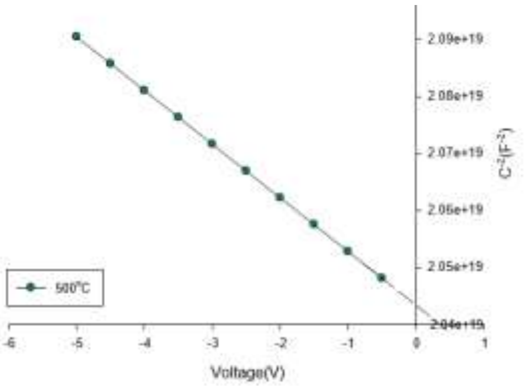


**Figure 10 (a).** 1/C$^2$-V Characteristic of Si-based tunnel diode at 500 °C

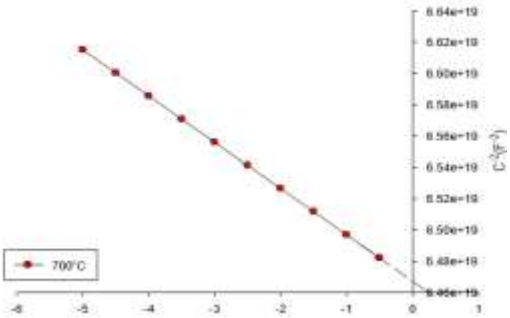


**Figure 10 (b).** 1/C$^2$-V Characteristic of Si- based tunnel diode at 600 °C

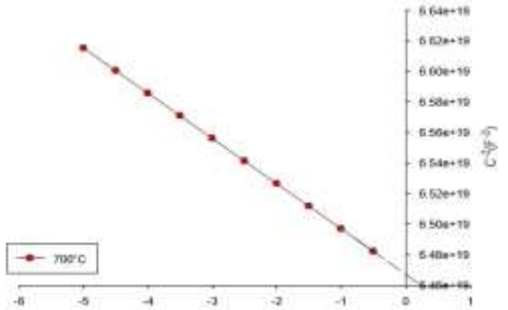


**Figure 10 (c).** 1/C$^2$-V Characteristic of Si- based tunnel diode at 700 °C

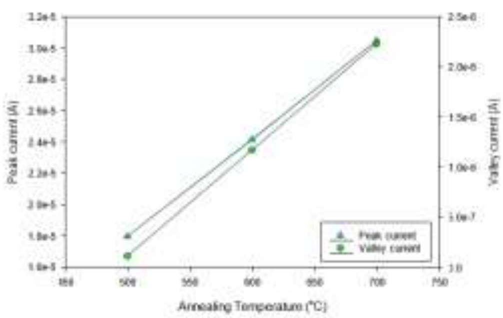


**Figure 11**. I-V Characteristics of Si based tunnel diode with $AL_2O_3$ layer at different annealing temperatures

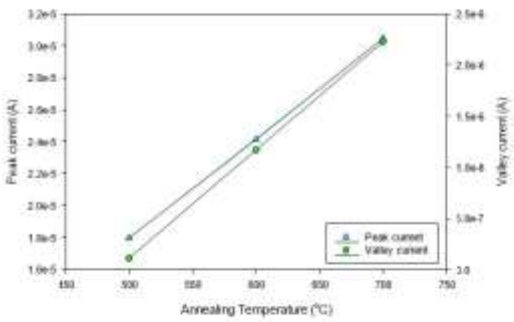


**Figure 12 (a).** The change in Peak current and Valley current as a function of different annealing temperatures

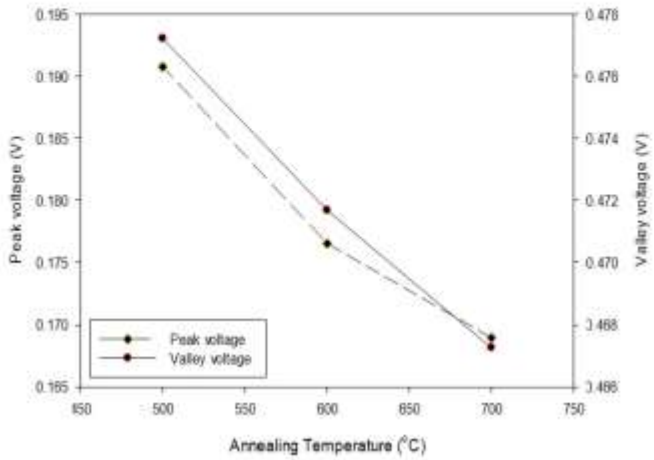


**Figure 12 (b).** The change in Peak voltages and Valley voltages as a function of different annealing temperatures

## Conclusion

As a result of XRD, the defect – free and prime- grade pattern was formed with hexagonal symmetry. The lattice distortion was determined to be 2.70 Å and lattice match was 98% to compared with $Al_2 O_3$ standard (c/a =2.73 Å). Two extra peaks were formed on XRD spectrum, and it might be attributed to the secondary oxide formation. The most intense peak was observed to be (024) plane and indicated the polycrystalline nature of $Al_2 O_3$. Thus, auto combustion method was quite suitable for $Al_2O_3$ powder preparation. It also confirmed the moisture- less powder of $Al_2O_3$.

As a result of powder analysis by SEM, homogeneous and uniform grains were formed. The grain size was examined to be 2.02 µm and it was porous structure. Therefore, it was concluded that the auto combustion route was quite feasible for ultrafine and moisture less powder fabrication. From the result of microstructure for $P_2O_5$ layer, it was clear that insulation layer was formed on p-Si (100) substrate at 1100 $^oC$. The film thickness was found to be 0.70 µm. As a result of SEM investigation for $Al_2O_3$ film, the image consisted of circular features known as rosette structure in microstructure. The temperature dependent of grain size for $Al_2O_3$film were 0.6, 0.5 µm and 0.43 µm respectively. It was found that grain size was more uniform at the increasing temperature 600 $^oC$ and 700 $^oC$. The film thickness was found to be 36.9 µm, 29.9 µm and 24.0 µm for the $Al_2O_3$ /$P_2O_5$/ $SiO_2$/ Si film at 500 $^{o}C$ ,600 $^{o}C$ and 700 $^{o}C$. The values were observed to be within the range of accepted value for "Thin Film".

As a result of charge conduction mechanism, C-2-V linear relationship was observed. It indicated the homogeneity of Al2O3 film. All built-in voltages were observed to be positive value and confirmed the p-type conductivity of silicon substrate. The smallest degree of depletion layer width was found at annealing temperature 500 oC. In addition, C-2 was directly proportional to W (depletion layer width). Thus, the Al2O3 layer was absolutely formed on SiO2/Si substrate at given annealing temperature. The experimental data resulted from this work indicated that the fabrication route and measurement system were quite feasible for low-cost tunnel device option. The growth mechanism used in this work was observed to be technically simple and easily adaptable. These results are much interesting for developing, application and optimizing in term of an improved device fabrication.

## Acknowledgements

The authors thank to Dr Tint Moe ThuZar, Rector, Yadanabon University for her motivation to have research-oriented mindset. The authors also thank to Pro-Rector Dr U Khin Myot, Pro-Rector Dr Myint Myint Oo and Pro-Rector Dr Khin Maw MawSoe, Yadanabon University, for their permission to do this paper. The authors also thank to Dr Khin Thida, Professor and Head of Physics Department, Yadanabon University, for her encouragement and valuable suggestion. The authors also acknowledge Dr Sandar Min, Professor of Physics Department, Yadanabon University, for her valuable advice and excellent supervision.

## References

Application Note 1369-1 2003 Solutions for Measuring Permittivity and Permeability with LCR Meters and Impedance Analyzers, Agilent Literature Number 5980-2862EN

Debasish S et al 2006 “Synthesis and characterization of sol-gel derived $ZrO_2$ doped $Al_2O_3$nano powder.” (India: Ceramic International)

Technical Overview 2003 Agilent 85071E Materials Measurement Software, Agilent literature number 5989-0222EN

https://www.Tunnel Diode.com